Raman and Rayleigh Scattering Diagnostics of a Two-Phase Hypersonic N_2 Flowfield

W. D. WILLIAMS* AND J. W. L. LEWIS†
ARO, Inc., Arnold Air Force Station, Tenn.

Theme

AS a result of interest both in producing and eliminating two-phase hypersonic flowfields, an improved understanding of homogeneous condensation processes is required. The desired experimental description of such two-phase flowfields includes the spatial location of condensation onset and the subsequent spatial growth rate of condensation. Additionally, the measurement of the gas density and temperature throughout the region of condensation onset and growth is desired. To this end, results of an experimental investigation of the homogeneous condensation of an N_2 flowfield are presented. Laser Rayleigh scattering was used to determine both the spatial location of condensation onset and its subsequent rate of growth. The depolarized Rayleigh scattering component was also measured throughout the condensation zone, and the results are used to infer properties of the aggregating molecular clusters. Finally, laser Raman scattering has been employed for the first time to determine both the gas density and temperature throughout the two-phase flowfield.

Contents

The condensing flowfield is assumed to be composed of a collection of gas monomers and molecular clusters, or i-mers, where i represents the number of molecules per cluster; further, n_i, α_i, and β_i are the number density, polarizability, and polarizability asymmetry factor, respectively, of the i-mer. For single scattering events the Rayleigh scattered intensity polarized parallel $\tilde{I}(\|)$ to the plane of polarization of the incident laser beam is[1]

$$\tilde{I}(\|) \simeq \sum_{i=1} (n_i/n_0)(\alpha_i/\alpha_1)^2 \tag{1}$$

where terms due to the polarizability asymmetry factors have been neglected; n_0 is the reservoir number density and the scattered intensity has been normalized to both the incident laser beam intensity and the scattered signal corresponding to a gas sample of number density n_0. The uncondensed, isentropic expansion gives

$$\tilde{I}(\|) \simeq (n_1/n_0)^0 \tag{2}$$

where superscript and subscript zeros denote the uncondensed, isentropic case and reservoir conditions, respectively. The axial variation of $\tilde{I}^0(\|)$ is provided by the method of characteristics solution (MOCS), and deviation of the measured $\tilde{I}(\|)$ from $\tilde{I}^0(\|)$ indicates the existence of an anisentropic process, which is condensation for this study.

For small values of condensate mass fraction $n_1 \simeq n_1{}^0 \simeq n_T$, where n_T is the total local number density, and the ratio of Eqs. (1) and (2) can be written as

$$f = [\tilde{I}(\|)/\tilde{I}^0(\|)] - 1 \simeq \sum_{i=2} X_i(\alpha_i/\alpha_1)^2 \tag{3}$$

where X_i is the i-mer mole fraction. Assuming small clusters to be characterized by weak chemical bonding, the cluster polarizability is assumed to be additive; i.e., $\alpha_i \simeq i\alpha_1$. Consequently, for a monodisperse distribution in cluster sizes $i = J$ and $\alpha_J \simeq J\alpha_1$, so that f is J^2X_J. The condensate mass fraction g is

$$g = JX_J/[1+(J-1)X_J] \tag{4}$$

The depolarization ratio ρ of the mixture of monomers and J-mers is the ratio of the measured scattered intensity components perpendicular and parallel to the incident plane of polarization; ρ is given by

$$\rho/\rho_1 = [1+(\rho_J/\rho_1)f]/(1+f) \tag{5}$$

where the depolarization ratios of the monomer and J-mer are ρ_1 and ρ_J, respectively, and ρ_1 is approximated by $\beta_1{}^2/15\alpha_1{}^2$. For significant condensation $f \gg 1$, and from Eq. (5) it is seen that $\rho \simeq \rho_J$, so a measurement of the depolarization ratio yields information regarding the cluster polarizability asymmetry.

For a laser beam of wavenumber $\bar{\nu}_0$ incident on vibrationally unexcited N_2 of number density n and rotational temperature T_R, the Stokes rotational Raman scattered intensity I_K from the Kth rotational energy level is related to the rotational quantum number K and T_R by[2]

$$I_K \propto n[\bar{\nu}_0 - 4B_0(K+3/2)]^4 \times \zeta(2K+1)S_K \exp[-K(K+1)\theta_R/T_R]/q_R \tag{6}$$

S_K is the scattering strength factor, $\theta_R = 2.86K$ and is the characteristic rotational temperature of N_2, and B_0 is the rotational constant. The rotational partition function q_R is accurately approximated by $T_R/2\theta_R$ when $T_R/\theta_R > 4$, and the spin statistics weighting factor ζ is two for even K and one otherwise for N_2. T_R is found using Eq. (6) and measured values of I_K by means of an iterative least-squares fitting to the I_K results as a function of $K(K+1)$. Further, the specie number density n is experimentally determined by summing the measured values of I_K over all observed transitions and employing an in-situ calibration for evaluation of the proportionality constant. The gas pressure P is an immediate experimental result using the product of n and T_R.

Consequently, measurements of $\tilde{I}(\|)$, ρ, the series of I_K values, and $\sum_{K=0} I_K$ yield information regarding the cluster size and concentration, the polarizability anisotropy of the clusters, T_R, n, and P for homogeneously condensing flowfields.

An underexpanded flowfield was produced using a movable 14.5° half-angle conical nozzle of 1.04 mm throat diameter (D) and exit area ratio of 13.4. The gas source was contained within and pumped by a cryogenically cooled chamber. The N_2 purity was 99.99%, and particulate filtering was employed to minimize heterogeneous condensation processes. The laser

Received April 3, 1974; synoptic received November 22, 1974; revision received January 2, 1975. Full paper available from National Technical Information Service, Springfield, Va., 22151, as AD-787675 at the standard price (available upon request). This work was sponsored by the Air Force Rocket Propulsion Laboratory (AFRPL), and the Air Force Systems Command (AFSC). The work was conducted by the Arnold Engineering Development Center (AEDC), AFSC, and results were obtained by ARO, Inc., contract operator of AEDC, Arnold Air Force Station, Tennessee.

Index categories: Multiphase Flows; Lasers; Research Facilities and Instrumentation.

* Physicist, Aerospace Projects Branch, von Kármán Facility.

† Senior Scientist, Aerospace Projects Branch, von Kármán Facility.

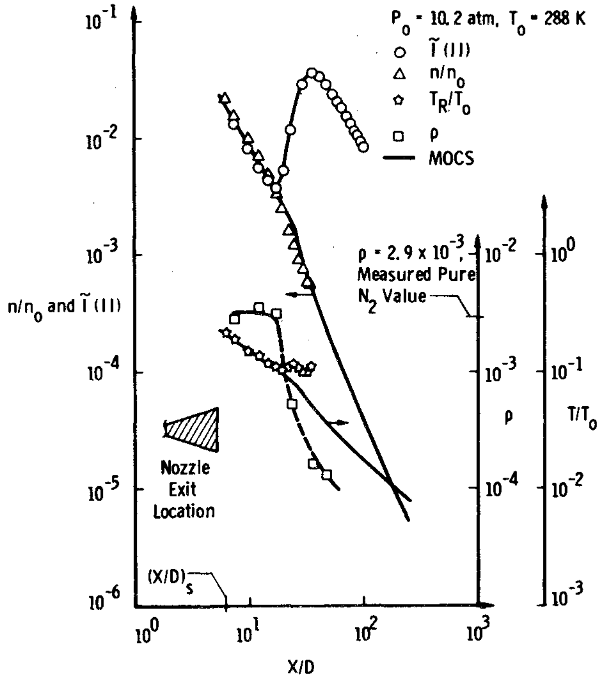

Fig. 1 Axial variation of Rayleigh/Raman results.

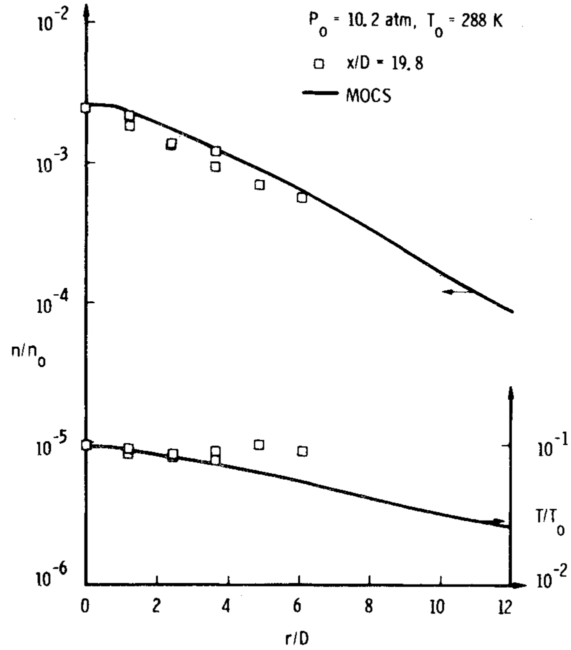

Fig. 2 Radial variation of Raman results.

source was operated at 514.5 nm at 1.5 w and 1.0 w for the Raman and Rayleigh measurements, respectively. The detection system consisted of an f/2 collection lens, a 0.85 m double grating spectrometer, a cooled EMI-9502B photomultiplier, and photon counting electronics. For the Rayleigh scattering measurements HN-22 Polaroid and a polarization scrambler also preceded the spectrometer in the optical train.

Figure 1 shows the axial variation of the Rayleigh scattering function $\tilde{I}(\|)$ and depolarization factor ρ; also shown is the axial profile of the Raman scattering results for n and T_R, and the MOCS predictions for n and T_R are indicated. For the reservoir conditions of $P_0 = 10.2$ atm and $T_0 = 288$K the axial locations X/D of the exit plane and saturation were 5.15 and 6.3, respectively. The axial variation of $\tilde{I}(\|)$ clearly shows condensation onset and growth as well as cessation of growth, after which the axial decay of $\tilde{I}(\|)$ varies approximately as $(X/D)^{-2}$. At the scattering peak $\tilde{I}(\|)$ exceeds $\tilde{I}^0(\|)$ by over two orders of magnitude. The ρ results prior to condensation onset are characteristic of monomeric N_2; the general trend of ρ through the onset and growth region of the cluster to a more symmetric scatterer is obvious and pleasing from the viewpoint of physical intuition. The n results show little, if any, effect from condensation, i.e., no significant depletion of the monomer is observed. Finally, the axial profile of T_R shows excellent agreement with the MOCS prior to onset, and the heating of the gas as a result of liberation of the heat of recombination resulting from the clustering process is clearly shown.

The radial profiles of n and T_R at the axial position $X/D = 19.8$ are shown in Fig. 2; the MOCS predictions are also shown. The off-axis discrepancies in both n and T_R relative to the MOCS are to be noted. Although centerline condensation has only just begun at $X/D = 19.8$, Fig. 2 shows significant off-axis heating which indicates that the spatial locus of condensation onset is two-dimensional in the axial and radial distances.

As discussed in Ref. 3, the assumption of a value of $g = 0.10$ for this particular flow is not unreasonable. Then, Eqs. (3) and (4) yield for the average cluster size $J \simeq 100$ and the condensate mole fraction $X_J \simeq 10^{-3}$. In conclusion, the feasibility of the application of Raman scattering density and temperature diagnostics to a two-phase N_2 flowfield has been initially demonstrated. Simultaneous Rayleigh scattering measurements obviously detect the onset and growth of condensation as well as cluster spatial symmetry changes.

References

[1] Lewis, J. W. L. and Williams, W. D., "Argon Condensation in Free-Jet Expansions," AEDC-TR-74-32, July 1974, Arnold Engineering Development, Arnold Air Force Station, Tenn.

[2] Placzek, G., "The Rayleigh and Raman Scattering," transl. from a publication of the Akademische Verlags Gesellschaft G.m.b.H., Leipzig, 1934, *Handbuch der Radiologie*, Heft 6, pp. 209–374.

[3] Lewis, J. W. L. and Williams, W. D., "Profile of an Anisentropic Nitrogen Nozzle Expansion," AEDC-TR-74-114, Nov. 1974, Arnold Engineering Development, Arnold Air Force Station, Tenn.